

Research Article

Cite this article: Hu C, An Y, Ma X, Feng X, Ma Y, Ma Y (2025) Resveratrol activates PGC-1 α pathway via PRAKK1 to regulate mitochondrial biogenesis and alleviate inflammatory responses in bovine mammary epithelial cells. *Animal Nutriomics* 2, e2, 1–13. <https://doi.org/10.1017/anr.2024.27>

Received: 25 August 2024

Revised: 2 December 2024

Accepted: 6 December 2024



Keywords:

PRKAA1; PGC-1 α ; resveratrol; inflammation; mitochondrial biogenesis

Corresponding author: Yanfen Ma;

Email: mayf@nxu.edu.cn

Resveratrol activates PGC-1 α pathway via PRAKK1 to regulate mitochondrial biogenesis and alleviate inflammatory responses in bovine mammary epithelial cells

ChunLi Hu , YanHao An, XueHu Ma, Xue Feng, Yun Ma and Yanfen Ma 

College of Animal Science and Technology, Key Laboratory of Ruminant Molecular and Cellular Breeding of Ningxia Hui Autonomous Region, Ningxia University, Yinchuan, China

Abstract

Mastitis in dairy cows is an important factor restricting the healthy development of dairy industry. Natural extracts have become a research hotspot to alleviate and prevent diseases because of their unique properties. The purpose of this study was to investigate the effects of resveratrol (RES) on the mitochondrial biosynthesis, antioxidation, and anti-inflammatory in bovine mammary epithelial cells (BMECs) and its mechanism involved. Blood samples were collected from six healthy cows and six mastitis affected cows, respectively, and lipopolysaccharide (LPS) was used to treat BMECs to construct inflammation models, gene interference is achieved by transfection. The results showed that messenger RNA (mRNA) expression of peroxisome proliferator-activated receptor γ coactivator-1 α (PGC-1 α) was down-regulated and mitochondrial biogenesis-related gene expression was disrupted in the blood of mastitis cows and LPS-induced BMECs. RES is the best active substance to activate PGC-1 α . The addition of RES can effectively alleviate the production of BMECs reactive oxygen species (ROS) and mitochondrial damage induced by LPS, and improve the antioxidation and anti-inflammatory ability, while the alleviation effect of RES is inhibited after interfering with protein kinase AMP-activated catalytic subunit α 1 (PRKAA1). In summary, our study emphasizes that PRKAA1 is a key gene mediating the activation of PGC-1 α by RES, which regulates mitochondrial biosynthesis, inhibits ROS release, attenuates mitochondrial damage, and improves mitochondrial antioxidant capacity through the activation of PGC-1 α by PRKAA1, thus attenuating the inflammatory response in BMECs.

Introduction

Clinical mastitis can lead to metabolic changes, decrease productivity and increase the elimination rate in lactating cows (Ballou 2012). It is the most common and expensive disease in dairy cows and usually occurs after calving (Zandkarimi et al. 2018). Mitochondrion, as the place where adenosine triphosphate (ATP) is produced, meets the energy demand of cells through oxidative phosphorylation system. Moreover, mitochondria are the energy centers of cells, which are very important to the life of eukaryotes (Annesley and Fisher 2019). Mitochondria are the main places where reactive oxygen species (ROS) are produced, which are essential to fight infection; however, excessive and uncontrolled production of ROS can become deleterious to the cell, leading to mitochondrial and tissue damage (Andrieux et al. 2021). Therefore, mitochondria are also central to the pro-inflammatory response and play a vital role in dealing with pathogenic infection (Missiroli et al. 2018). Mitochondria are highly dynamic organelles that undergo a coordinated cycle of fission and fusion, known as “mitochondrial dynamics.” Imbalanced mitochondrial dynamics are associated with a range of diseases that are broadly characterized by impaired mitochondrial function and increased cell death (Whitley et al. 2019). Research has found that the Xuanfei Baidu formula exerts anti-inflammatory effects by restoring mitochondrial kinetics and reducing the activation of inflammasomes (Li et al. 2023).

Peroxisome proliferator-activated receptor γ co-activation factor-1 α (PGC-1 α) is a co-transcriptional regulator that is a major factor in the regulation of mitochondrial biogenesis and function (Rius-Pérez et al. 2020). PGC-1 α is an important node connecting metabolic regulation, redox control, and the inflammatory pathway; its maladjustment changes redox homeostasis in cells and aggravates inflammatory reaction, usually accompanied by metabolic disorder (Eisele and Handschin 2014). In the process of inflammation low-level PGC-1 α downregulates the expression of mitochondrial antioxidant genes, induces oxidative stress and

© The Author(s), 2025. Published by Cambridge University Press on behalf of Zhejiang University and Zhejiang University Press. This is an Open Access article, distributed under the terms of the Creative Commons Attribution licence (<http://creativecommons.org/licenses/by/4.0>), which permits unrestricted re-use, distribution and reproduction, provided the original article is properly cited.

promotes the activation of nuclear factor- κ B (NF- κ B), PGC-1 α regulates the expression of mitochondrial antioxidant genes, including catalase, peroxidase 3 and 5, uncoupling protein 2 (UCP2), and thioredoxin reductase, to prevent oxidative damage and mitochondrial dysfunction (Das *et al.* 2021). The AMP-activated protein kinase (AMPK)/PGC-1 α pathway plays an important role in regulating mitochondrial biogenesis (Li *et al.* 2016). The protein kinase AMP-activated catalytic subunit α 1 (PRKAA1) the catalase that plays a key role in regulating cell energy metabolism via phosphorylation, and PRKAA1 has been found to be related to inflammatory (Krishan *et al.* 2014; Yang *et al.* 2022c). Zhu *et al.* (Zhu *et al.* 2014) found that PRKAA1 mediated the clearance of damaged mitochondria in cells, which is necessary for cell maturation and homeostasis.

Resveratrol (RES) is a polyphenol found in grapes, mulberry trees, peanuts, rhubarb, and other plants, which plays a beneficial role in preventing chronic diseases related to inflammation, and participates in regulating cell processes, such as gluconeogenesis, lipid metabolism, mitochondrial biogenesis, angiogenesis, and apoptosis (Malaguarnera 2019; Meng *et al.* 2021). Research has indicated that RES could inhibit microcirculation disorder by activating the sirtuin1 (SIRT1)-forkhead box O1 (FOXO1) axis, thus relieving the acute pancreatitis in rats (Rong *et al.* 2021). Kong *et al.* (Cong *et al.* 2021) found that RES improved mouse steatohepatitis by regulating the mmu-miR-599/pregnane X receptor pathway to inhibit the related inflammatory factors. RES can reduce mitochondrial damage caused by some stress sources, trigger mitochondrial biogenesis and improve the mitochondrial-related bioenergy state in mammalian cells (Jardim *et al.* 2018). Research has shown that RES inhibits apoptosis and oxidative stress of bovine mammary epithelial cells (BMECs) induced by aflatoxin B1 and participates in the Nrf2 signaling pathway (Zhou *et al.* 2019). RES also improves granular cell activity through mitochondrial biogenesis (Grive and Sauerbrun-Cutler 2021). Previous studies have shown that RES can reduce lipopolysaccharide (LPS)-induced inflammatory response via PGC-1 α , but the specific molecular regulatory mechanism remains unclear (Huang *et al.* 2021; Xiao-Li *et al.* 2017). This study aims to investigate how RES activates PGC-1 α to regulate mitochondrial biosynthesis and alleviate the inflammatory responses in BMECs and to provide basic data for subsequent research on RES relieving dairy cows with mastitis.

Materials and methods

Animal ethics

The Animal Experiment Committee of Ningxia University approved the experimental procedures in line with China's Regulations for the Administration of Affairs Concerning Experimental Animals (Ningxia University Ethics No. 22–72). These procedures were rigorously followed according to the approved guidelines. Ningxia Xin'ao Agricultural Farm authorized the use of these animals in the study.

Collection of cows and blood samples

The experimental cows came from an intensive dairy farm in Yingchuan (Ningxia, China). The cows were divided into healthy cows ($n = 6$) and mastitis cows ($n = 6$), according to the California mastitis test method. Then, 10 mL of tail root venous blood was collected from each cow. The serum was separated after centrifugation (3,000 g, 15 min) and stored at -80°C for subsequent ELISA

detection. Information on healthy and mastitis cows is presented in **Supplementary Table 1**.

Construction of the inflammatory BMECs

The BMECs cell lines used in this study were obtained from laboratory researchers frozen in liquid nitrogen (Yang *et al.* 2022b). BMECs were spread into a six-well plate. They were washed twice with phosphate buffered saline (PBS) (Hyclone, USA) and replaced with a new medium when the cell density reached 60 ~ 70% confluency. Then, 105 μL of LPS was added to each well to achieve a final concentration of 50 ng/ μL (Strandberg *et al.* 2005), thereby inducing inflammation. Cells extracts were collected in centrifuge tubes following disruption with TRIzol at the 0, 3, 6, 12, and 24 h after induction, and stored at -80°C for RNA extraction.

BMECs culture and treatment

The BMECs were spread into a six-well plate, and the cells were treated when the cell density reached 70–80%. The transfection reagent was Lipofectamine 3000 (Invitrogen, Thermo Fisher Scientific, USA). Interfering fragments refer to small molecules interfere with RNA fragments (siRNA), siRNA and homologous target RNA complement each other, and specific enzymes degrade target RNA, thus inhibiting and down-regulating gene expression. Three interfering fragments and one control fragment (Negative control) of PRKAA1 gene were designed and synthesized, the interfering fragment sequences are shown in **Supplementary Table 2**. The interference fragment was synthesized by Shengggong Bioengineering Co., Ltd. (Shanghai, China). The cell treatment in each experimental group was as follows: LPS group: 105 μL (final concentration was 50 ng/ μL) LPS (Sigma, USA) was added for the group; si-PRKAA1 group: the PRKAA1 interference fragment was transfected according to the instruction of Lipofectamine 3000, and the cells were collected after transfection for 48 h; RES + si-PRKAA1 group: BMECs were treated using 15 $\mu\text{mol/L}$ RES (G-clone, China) for 12 h after the PRKAA1, and the interference fragment was transferred into the BMECs for 36 h; LPS + si-PRKAA1 group: BMECs were treated using 50 ng/ μL LPS for 12 h after the PRKAA1, interference fragment was transferred into the BMECs for 36 h; LPS + RES + si-PRKAA1 group: BMECs were treated with 15 $\mu\text{mol/L}$ RES for 12 h and then treated with 50 ng/ μL LPS for 12 h after the PRKAA1 interference fragment was transferred into the BMECs for 24 h.

Real-time fluorescence quantitative PCR (qPCR)

RNA was extracted from BMECs, and blood was extracted using the Trizol (Takara, Japan) method. The integrity of the RNA was detected using gel electrophoresis, and the quality and concentration of RNA were detected using a multifunctional full-wavelength enzyme-labeled instrument (SYNERGY LX, Bio-Rad, USA) (He *et al.* 2024). The complementary DNA (cDNA) was obtained by the reverse transcription of RNA with a reverse transcription reagent (Takara, Japan). The qPCR (CFX96, Bio-Rad, USA) system was as follows: consisted of 7.5 μL of 2 \times SYBR green qPCR mix, 1.5 μL of cDNA, 0.3 μL of each primer (upstream and downstream), and 5.4 μL of deionized water. Glyceraldehyde-3-phosphate dehydrogenase (GAPDH) was selected as the internal reference gene. Primer information is shown in **Supplementary Table 3**; primers were synthesized by General Biology Co., Ltd. (Anhui, China).

Nucleoplasm separation and ELISA

The nuclear-cytoplasmic separation kit (Invitrogen, Thermo Fisher scientific, USA) was used for nuclear-cytoplasmic separation of BMECs. The mass of nuclear-mass separation was detected via 1% gel electrophoresis, assessed the quality of RNA separation between the nucleus and cytoplasm, and reverse transcription was performed to produce cDNA. Semiquantitative detection was used to analyze the expression levels of PGC-1 α , PRKAA1, Tfam, dynamin-related protein (Drp1), Fis, Mfn1, and Mfn2 in both compartments, followed by gel electrophoresis to measure each gene's expression in the nucleus and cytoplasm. Gray analysis was performed with Image J (version v10.6.2) (Strandberg et al. 2005) online software. The BMECs medium supernatant (or blood) from each treatment group was collected and tested for the secretion of cytokines interleukin 6 (IL-6) and interleukin 8 (IL-8) according to the ELISA kit (Ruixin, Quanzhou, China) instructions. Detection of malondialdehyde (MDA) content according to MDA kit (Ruixin, Quanzhou, China) instructions.

Bioinformatics analysis

The protein sequence of PRKAA1 and PGC-1 α was obtained in NCBI, and the potential phosphorylation site of PGC-1 α was predicted using NetPhos 3.1 online software. Protein phosphorylation analysis software Scansite was used to predict the protein kinase that can phosphorylate PGC-1 α (Ma et al. 2018). The hydrophilicity and hydrophobicity of the PRKAA1 protein were analyzed using ProtScal (Wilkins et al. 1999) online software, the secondary structure of PRKAA1 protein was analyzed using SOPMA, and the tertiary spatial configuration of PRKAA1 protein was obtained using SWISS-MODEL (Waterhouse et al. 2018). See **Supplementary table 4** for the web addresses of the online sites.

Flow cytometry

For flow cytometry, cells were processed according to the apoptosis kit instructions. In brief, adherent cells were washed with PBS and treated with trypsin to digest them for 3 min. Then, cell culture medium was added to terminate the digestion, followed by the centrifugation of the medium at 1 000 \times g for 5 min and discarding of the supernatant. Next, 1 mL LPS was added to resuspend the cells, and the suspension was again centrifuged at 1000 \times g for 5 min. The supernatant was discarded and 195 μ L of AnnexinV-FITC binding solution and 5 μ L AnnexinV-FITC were added and mixed gently. Finally, 10 μ L propidium iodide staining solution was added and mixed, followed by incubation in the dark for 10–20 min at room temperature. The stained cells were subjected to flow cytometry. Cells were processed according to the apoptosis kit instructions (Beyotime, Shanghai, China) (Hu et al. 2024).

Western blot

Protein was extracted according to the instructions of the whole protein extraction kit (KeyGEN BioTECH, Nanjing, China). In total, 200 μ L of the mixtures were added into six-well plates for protein extraction. Proteins were quantified using the bicinchoninic acid (BCA) protein detection kit (KeyGEN BioTECH, Nanjing, China). Dilute and adjust the protein sample to the same amount, add the loading buffer (Yamei, Shanghai), and then boil at 100°C for 10 min. 1.00 mm minigel was prepared according

to the kit instructions of the enzyme PAGE gel rapid preparation kit (Yamei, Shanghai). The gels were used to separate the proteins via electrophoresis, and the electrophoretic positions of the protein bands were compared with a 10–250-kDa prestained protein marker (Yamei, Shanghai). The separated proteins were transferred to polyvinylidene fluoride (PVDF) membranes (Millipore, USA). After transfer, the membranes were incubated with a rapid sealing solution (Yamei, Shanghai) for 15 min, followed by washing with tris buffered saline-tween-20 (TBST) (Servicebio, Wuhan) solution and overnight incubation in TBST solution containing primary antibodies primary antibody information was as follows: GAPDH (Abways, AB0036, 1:1 000), Tfam (Abways, CY7172,1:1 000), Fis (Abways, CY8730,1:1 000), PGC-1 α (Abcam, ab54481, 1:1 000), Mfn2 (Abcam, ab56889, 1:1 000), Bax (Abways, CY5059,1:1 000), Caspase-3 (Beyotime, AC030, 1:1 000). After incubation with primary antibodies, the membrane was washed with TBST thrice for 10 min each time. Subsequently, the membranes were incubated with horseradish peroxidase (HRP)-coupled secondary antibodies (HRP-labeled goat trypsin antibodies, 1 : 20 000 Shenggong, Shanghai) for 2 h. Finally, the membrane washed thrice with TBST for 10 min each time and imaged using a chemiluminescence imaging system (Tanon-5200, Shanghai) after treatment with an enhanced chemiluminescence (Yamei, China) reagent.

Mitochondrial membrane potential and ROS detection

Mitochondrial damage was assessed using a mitochondrial membrane potential assay kit (Beyotime, China). Briefly, the cells in the six-well plate were allowed to grow to 70–80% confluency, and the medium in the six-well plate was discarded and the cells washed with PBS for 1–2 times. Then, 1 mL of medium and 1 mL of JC-1 staining working solution were added to each well, respectively, and they were fully and uniformly mixed and placed in an incubator at 37°C and 5% CO₂ for 20 min. After the incubation, the mixture was discarded, and 2 mL precooled JC-1 staining buffer was added into each well twice for 3 min each time. Then, 2 mL medium was added to each well to avoid light and photographed using a fluorescence inverted microscope after the staining buffer was discarded. The content of ROS in cells was detected using an ROS kit (Lablead, China). Briefly, the cells in the six-well plate were allowed to grow to 70–80%, and the medium in the six-well plate was discarded and washed with PBS 1–2 times. Then, 1 mL diluted 2',7'-Dichlorodihydrofluorescein diacetate (DCFH-DA) was added into each well to be fully and uniformly mixed and placed in an incubator at 37°C and 5% CO₂ for 20 min. At the end of the incubation, DCFH-DA was discarded, and 2 mL serum-free medium without antibody was added into each well for washing 3 times, for 3 min each time, in the dark. The pictures were taken under a fluorescence inverted microscope.

Data analysis

For each group, at least three independent experiments were performed. The qPCR results of fluorescence quantification were analyzed using the $2^{-\Delta\Delta Ct}$ method, and the data are expressed as mean \pm standard error. Each test ensures three independent technical repeats. T-test for significance of experimental data was performed using GraphPad Prism 8 software. $P < 0.05$ (*), and $P < 0.01$ (**) indicated statistical significance. The protein band grayscale was analyzed using the Image J software.

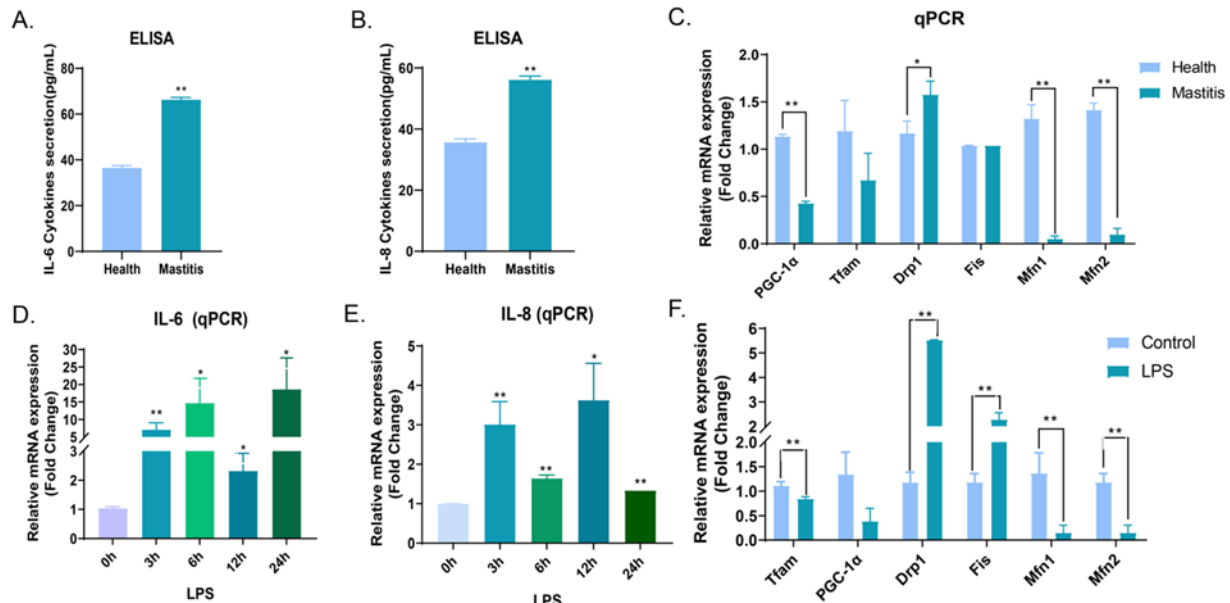


Figure 1. Activation disorders of PGC-1 α in dairy cows with mastitis. A–B. The content of the IL-6 and IL-8 in the blood of dairy cows with mastitis. C. The mRNA expression of PGC-1 α , Tfam, Drp1, Fis, Mfn1, and Mfn2 in the blood of mastitis cows. D–E. The mRNA expression of IL-6 and IL-8 in BMECs induced by LPS for 0, 3, 6, 12, and 24 h. F. The mRNA expression of PGC-1 α , Tfam, Drp1, Fis, Mfn1, and Mfn2 in BMECs induced by LPS. * $P < 0.05$, ** $P < 0.01$.

Results

Activation disorders of PGC-1 α in dairy cows with mastitis

In order to clarify the relationship between PGC-1 α and mastitis, the mRNA expression level of PGC-1 α in blood was detected in healthy and mastitis dairy cows. The protein expression levels of inflammatory factors in the blood of healthy cows and mastitis cows were detected with ELISA (Fig. 1A and Fig. 1B). qPCR was used to measure the mRNA expression levels of inflammatory factors and mitochondrial biosynthesis-related genes in the blood of both healthy and mastitis-affected cows (Fig. 1C). The results showed that compared with healthy cows, the content of IL-6 (Fig. 1A, $P < 0.01$) and IL-8 (Fig. 1B, $P < 0.01$) in the blood of mastitis cows increased significantly, and the mRNA expression level of the PGC-1 α gene was significantly decreased (Fig. 1C, $P < 0.01$); Compared with healthy cows, the mRNA expression levels of transcription factor A (Tfam), mitofusin 1 (Mfn1), and mitofusin 2 (Mfn2) in the blood of mastitis cows were downregulated, while the mRNA expression level of Drp1 was upregulated (Fig. 1C, $P < 0.01$). LPS was used to induce BMECs for 0, 3, 6, 12, and 24 h, and the results showed that the mRNA expressions of inflammatory factors (IL-6 and IL-8) in each time period were all higher than 0 h, indicating that the inflammatory model was successful constructed (Fig. 1D–E, $P < 0.05$). The mRNA expression of PGC-1 α and mitochondrial biogenesis genes (Tfam, Mfn1, Mfn2, Drp1, and fission, Fis) in inflammatory cells was detected. In contrast to the control group, the mRNA expression levels of PGC-1 α , Tfam, Mfn1, and Mfn2 in inflammatory cells decreased, whereas the mRNA expression levels of Drp1 and Fis mRNA increased. (Fig. 1F, $P < 0.01$).

PRKAA1 is a PGC-1 α -phosphorylated kinase

To further screen proteins related to PGC-1 α phosphorylation, the NetPhos 3.1 server was used to predict the existence of 129 potential phosphorylation sites of the protein, and the results showed

that the main phosphorylated amino acids were serine (Ser), threonine (Thr) and tyrosine (Supplementary Fig. 1A). Meanwhile, the protein phosphorylation analysis software Scansite was also used to predict the protein kinase that might phosphorylate PGC-1 α (Supplementary Figure 1B), and the results showed that the protein kinase with the highest score was PRKAA1, which targeted 254 Thr (T254) on PGC-1 α (Supplementary Table 5). In addition, we used SOPMA online software to predict the secondary structure of the PRKAA1 protein. It was found that the PRKAA1 protein mainly was consisted of α -helix (32.75%, indicated by the blue vertical line), irregular curl (44.08%, shown by the purple short line), a small number of extended chains (red middle vertical line area, 16.38%) and β -corner (green middle vertical line area, 6.79%; Supplementary Figure 1C). The hydrophobicity of the protein was analyzed using ProtScal, which showed that amino acid hydrophobic residues accounted for a large proportion of the PRKAA1 protein (Supplementary Figure 1D). SWISS-MODEL was used to predict the tertiary structure of PRKAA1, and the results showed that most of the protein had an irregular curl and α -helix structure, which was consistent with the secondary structure prediction results (Supplementary Figure 1E).

PRKAA1 activates PGC-1 α to regulate mitochondrial biogenesis

The activation of PRKAA1 on PGC-1 α was further determined, and the mRNA expression of PRKAA1 in the blood of mastitis cows was detected using qPCR. The results showed that the mRNA expression of PRKAA1 in mastitis cows was decreased compared to that in healthy cows (Fig. 2A, $P < 0.01$). Subsequently, we designed three interfering fragments specific for the PRKAA1 gene and selected si-PRKAA1-1384 as the best interfering fragment (Fig. 2B, $P < 0.01$). In contrast to the control group, the mRNA levels of PGC-1 α , Tfam, Mfn1, and Mfn2 was down-regulated, while the mRNA expression of mitochondrial fission genes (Drp1 and Fis) was upregulated after PRKAA1 interfered (Fig. 2C, $P < 0.05$), which shows that mitochondrial biogenesis

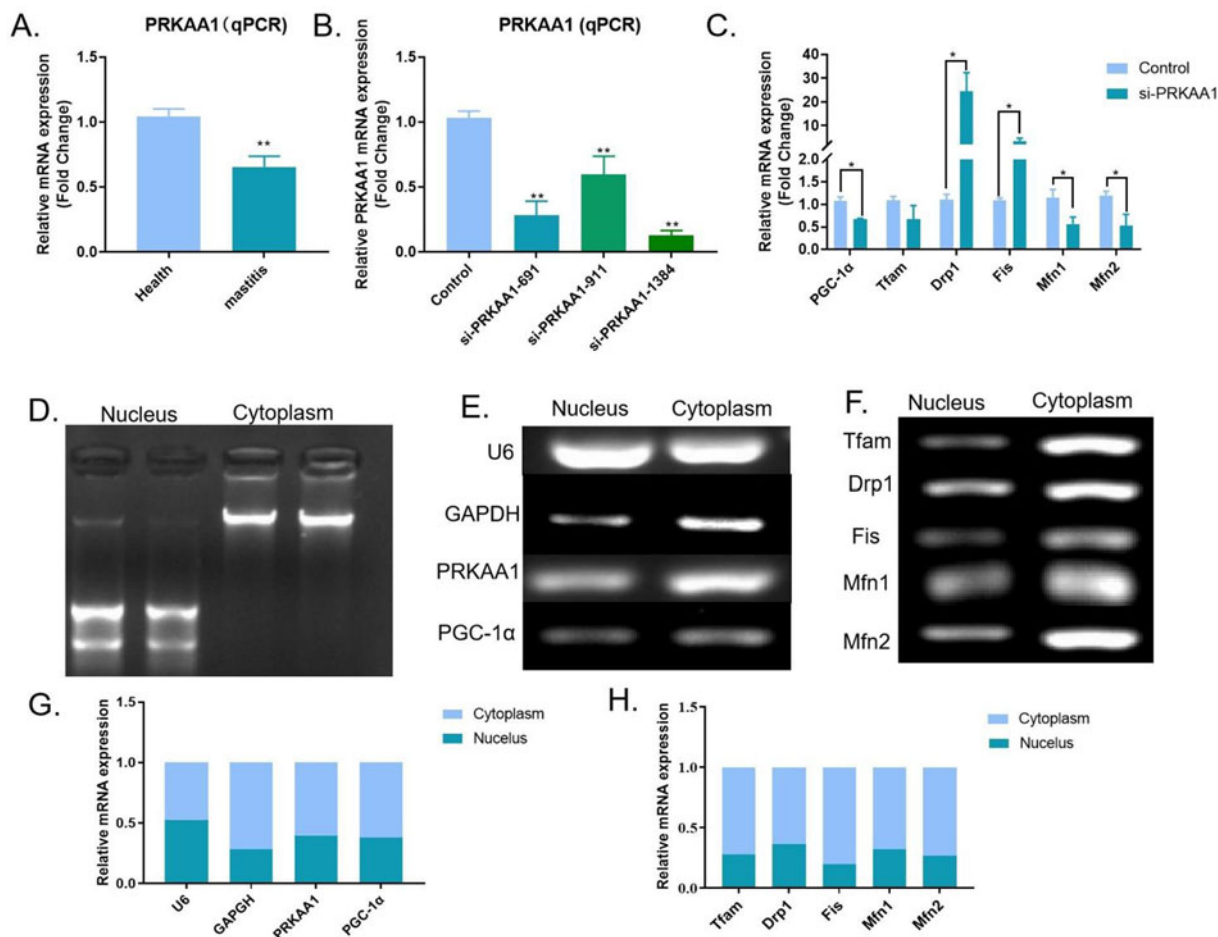


Figure 2. PRKAA1 activates PGC-1 α to regulate mitochondrial biogenesis. A. The mRNA expression of PRKAA1 in blood of healthy cows and mastitis cows. B. Screening of interfering fragments of PRKAA1 gene. C. The mRNA levels of PGC-1 α , Tfam, Drp1, Fis, Mfn1, and Mfn2 in BMECs treated with the PRKAA1 interference fragment were measured by qPCR. D. Detection of RNA isolated from nuclear and cytoplasm of BMECs using gel electrophoresis. E–F. Semi-quantitative detection of PRKAA1, PGC-1 α , Tfam, Drp1, Fis, Mfn1, and Mfn2 localization. G–H. Image J was used to quantify the gel electrophoresis patterns of each gene. * $P < 0.05$, ** $P < 0.01$.

is disordered. The nuclear localization of PGC-1 α and mitochondrial biogenesis-related genes (Tfam, Mfn1, Mfn2, Drp1, and Fis) results showed that they were mainly located in the cytoplasm (Fig. 2D–H).

RES activates PGC-1 α via PRKAA1

To find the optimal active substance to activate PGC-1 α , four compounds were tested simultaneously. The BMECs were treated with RES (non-flavonoid polyphenol organic compounds), tea polyphenols (the main component is catechin compounds), lycopene (LYC, a carotenoid found in plant foods) and tartary buckwheat (TB, the main component is flavonoids) extract for 12 h (the final concentrations were all 15 $\mu\text{mol/mL}$), and the cells were collected, respectively. The mRNA expression of PGC-1 α in the four treatment groups was detected using qPCR. The results found that all four substances significantly increased the mRNA expression of PGC-1 α , and the mRNA levels of PGC-1 α were the highest in BMECs treated with RES (Fig. 3A, $P < 0.01$). The above results showed that RES was the best activator of PGC-1 α . In order to further prove that RES activates PGC-1 α through PRKAA1 to regulate mitochondrial biosynthesis, BMECs were treated with RES

for 12 h after the PRKAA1 interference fragment was transfected into BMECs for 36 h. The results showed that the mRNA expression of PGC-1 α increased significantly in BMECs treated with RES but decreased in BMECs in which PRKAA1 was targeted (Fig. 3B, $P < 0.05$) compared with the control group. This indicates the activation efficiency of RES on PGC-1 α without PRKAA1. At the same time, the mRNA expressions of mitochondrial synthesis genes and mitochondrial fission genes were detected. The results showed that the addition of RES promoted the mRNA expressions of the mitochondrial synthesis genes (Tfam, Fig. 3C; Mfn1, Fig. 3F; Mfn2, Fig. 3G; $P < 0.01$) and anti-apoptosis genes (B cell lymphoma protein-2, Bcl-2; Fig. 3J, $P < 0.05$), and RES inhibited the mRNA expressions of the mitochondrial fission genes (Drp1, Fig. 3D; Fis, Fig. 3E; $P < 0.01$) and pro-apoptosis genes (Caspase-3, Fig. 3H; Bax, Fig. 3I; $P < 0.01$). However, the mRNA expression of the mitochondrial synthesis gene and anti-apoptosis gene was significantly inhibited, and the mRNA expression of the fission and apoptosis gene was promoted by adding RES after interfering with PRKAA1 (Fig. 3B–I, $P < 0.01$). A western blot was used to detect the protein expressions of the mitochondrial synthesis gene (Tfam), fission gene (Fis), and apoptosis gene (Caspase3 and Bcl-2 associated X, Bax), and the protein expression results tended to be consistent with those of the qPCR (Fig. 3K). The

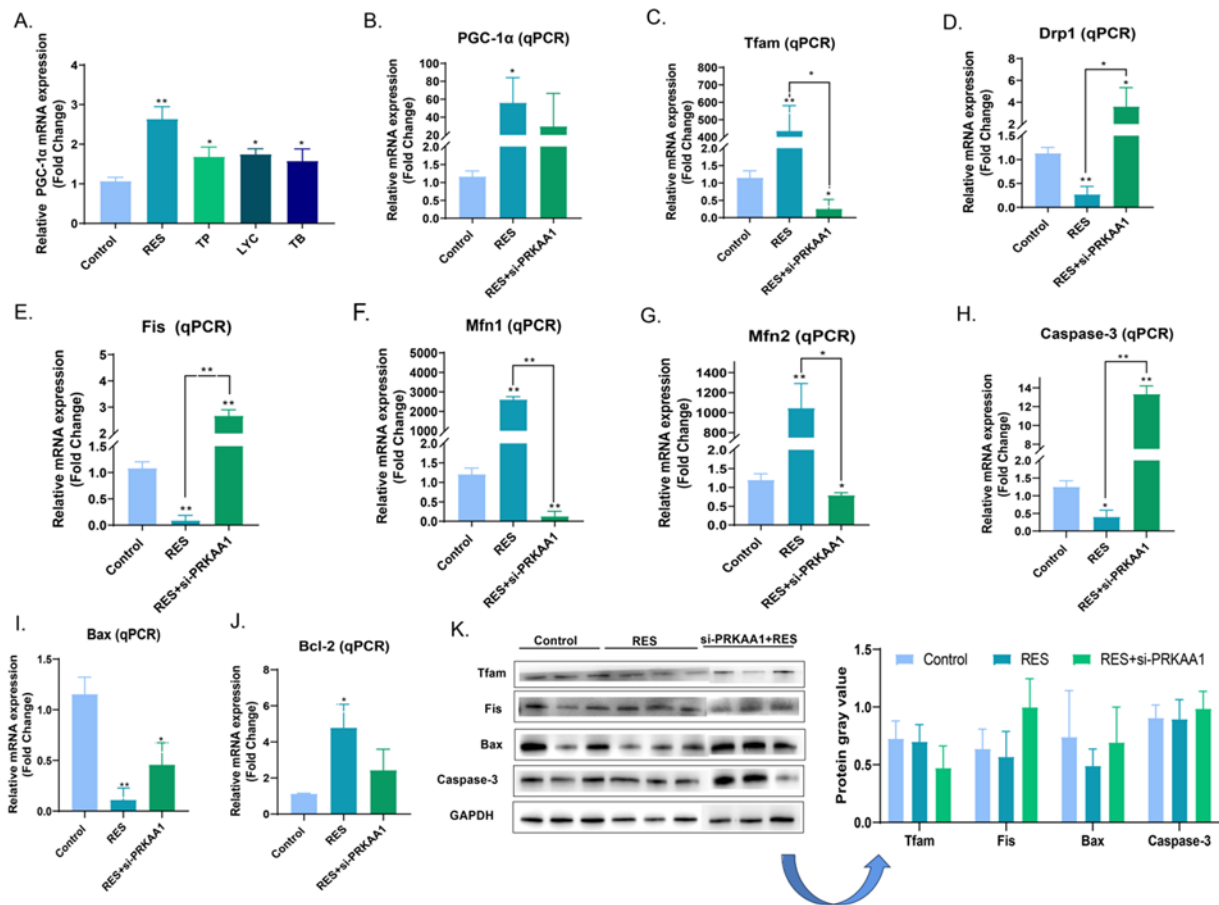


Figure 3. RES activates PGC-1 α via PRKAA1. A. BMECs were treated with RES, TP, LYC, and TB for 12 h, and the final concentration was 15 μ mol/L. B–J. The mRNA levels of PGC-1 α , Tfam, Drp1, Fis, Mfn1, Mfn2, Caspase-3, Bax, and Bcl-2 in control group, RES group and RES + si-PRKAA1 group. K. Western blot. * $P < 0.05$, ** $P < 0.01$.

mitochondrial membrane potential of cells in three experimental groups was detected, and the results showed that the red fluorescence intensity of the mitochondria in RES + si-PRKAA1 group was weaker than that of in the RES group, indicating that the protective effect of RES on mitochondria was weakened after interfering with PRKAA1 (Fig. 4A, Supplementary Figure 2A). The results of ROS detection showed that the ROS content in the RES + si-PRKAA1 group was higher than that of in the RES group (Fig. 4B, Supplementary Figure 2B), while the results of flow cytometry showed that there was no significant difference in apoptosis among the three experimental groups (Fig. 4C, Supplementary Figure 2C). In summary, the PRKAA1 is a key gene that can mediate RES to activate PGC-1 α , and it can also regulate the mitochondrial biogenesis and the expression of genes related to mitochondrial function.

ES regulate mitochondrial biosynthesis to reduce mitochondrial damage and alleviate apoptosis in inflammatory BMECs by activating the PRKAA1

We further explored the effect of PRKAA1-mediated RES on the mitochondrial biosynthesis in inflammatory BMECs. The results showed that the mRNA expression of PGC-1 α was significantly downregulated in BMECs induced by LPS and upregulated after

adding RES, compared with the control group, indicating that RES significantly increased the mRNA expression of PGC-1 α in BMECs induced by LPS. RES did not increase the mRNA levels of PGC-1 α in BMECs induced by LPS after interfering with si-PRKAA1, which shows that the promotion efficiency of RES was dependent on the PRKAA1 (Fig. 5A, $P < 0.05$) compared with the control group. Similarly, the mRNA levels of the mitochondrial synthesis genes (Tfam, Mfn1 and Mfn2) were inhibited in BMECs induced by LPS. The mRNA expression could be promoted by RES, but the promotion effect of RES was not obvious after interfering with PRKAA1 (Fig. 5B–D, $P < 0.05$). Meanwhile, the mRNA expression of mitochondrion fission genes (Drp1 and Fis) was increased significantly in the inflammatory state, and the expression was inhibited after adding RES. However, the inhibition effects of RES were weakened after interfering with PRKAA1 (Fig. 5E–F, $P < 0.05$) and the mRNA expressions of the apoptosis gene and anti-apoptosis gene were also detected, the findings indicated that the mRNA levels of the apoptotic genes promoted in BMECs induced by LPS, and the mRNA expression could be inhibited by RES, but the promotion effect of RES was not obvious after interfering with PRKAA1. The mRNA expression of the anti-apoptosis gene showed the opposite result (Fig. 5G–I, $P < 0.01$). A western blot was used to detect the protein expressions of a mitochondrial synthesis gene (Tfam), fission gene (Fis), and apoptosis gene (Caspase-3 and Bax), and the results were consistent with

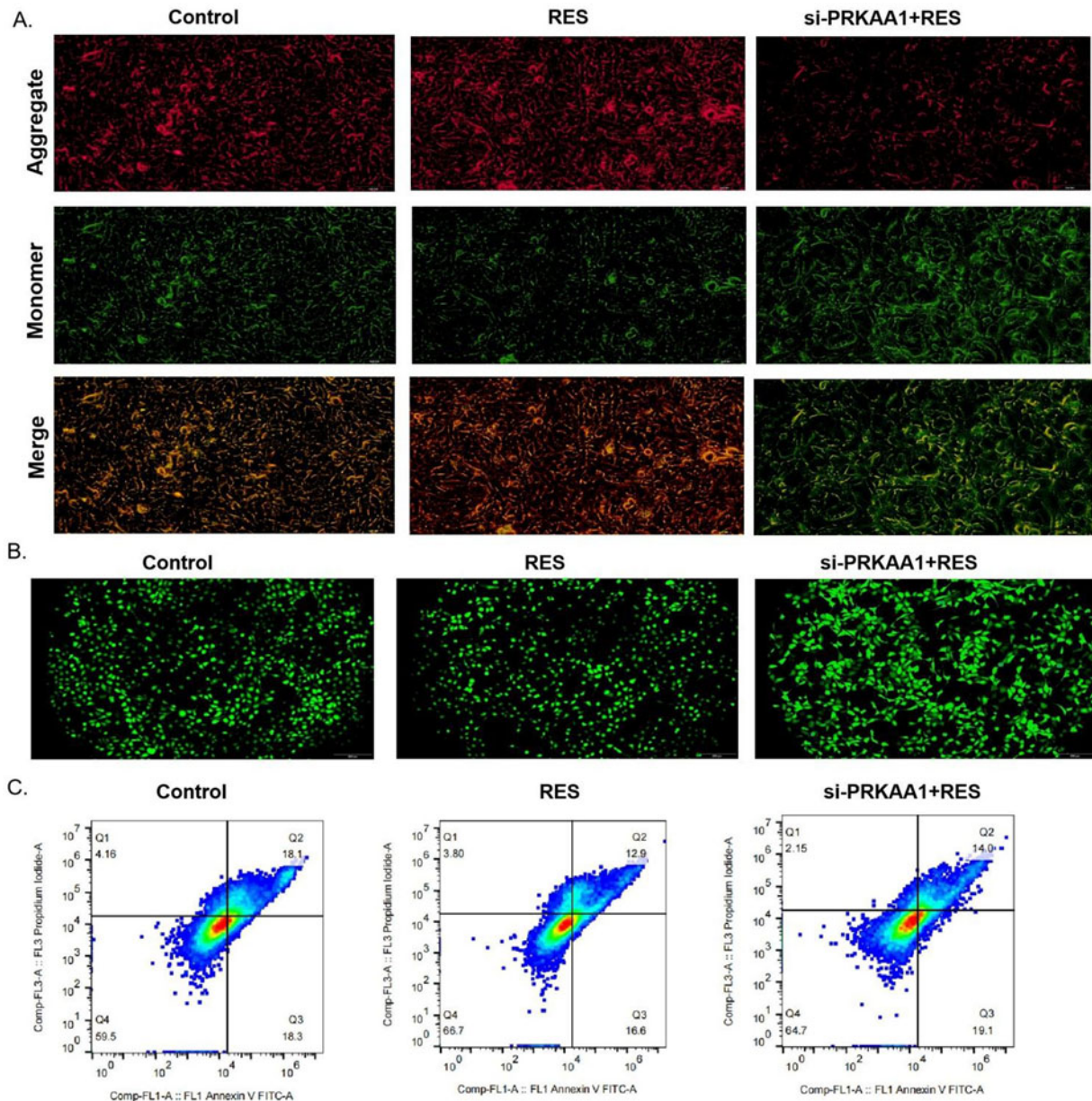


Figure 4. RES activates PGC-1 α via PRKAA1 relieve mitochondrial damage in inflammatory BMECs, reduce ROS release, and inhibit cell apoptosis. A. Mitochondrial membrane potential detection with JC-1. B. ROS detection with ROS detection kit. C. Apoptosis was detected using flow cytometry. * $P < 0.05$, ** $P < 0.01$. Scale bar = 200 μm .

those of qPCR (Fig. 6A). The results of mitochondrial membrane potential showed that the red fluorescence intensity in the LPS group was significantly reduced compared with the control group, indicating that mitochondria were seriously damaged, while the red fluorescence in the RES + LPS group was stronger than that of in the LPS group, indicating that RES had the protective effect on mitochondria, and the protective effect of RES on mitochondria was weakened after interfering with PRKAA1 (Fig. 6B, Supplementary Figure 2D). Apoptosis was detected using flow cytometry, and we found that apoptosis in the RES + LPS group was lower than that in the LPS group, but increased after interfering with PRKAA1 (Fig. 6C, Supplementary Figure 2E). Therefore, the above results show that PRKAA1 could mediate RES to promote mitochondrial biosynthesis in BMECs induced by LPS, and

reduced mitochondrial damage and alleviated the apoptosis of BMECs.

RES improve antioxidant and anti-inflammatory capacity in inflammatory BMECs by activating the PRKAA1

On the basis of the above research, the anti-inflammatory mechanism of PRKAA1-mediated RES was explored. In contrast to the control group, the mRNA levels of the oxidative gene MDA ($P < 0.01$) in BMECs induced by LPS was increased significantly, and inhibited after BMECs treated with RES, but was not significantly inhibited after interfering with PRKAA1 (Fig. 7A, $P < 0.05$). However, the mRNA levels of antioxidant genes (superoxide dismutase, SOD, Fig. 7B, $P < 0.05$; glutathione peroxidase,

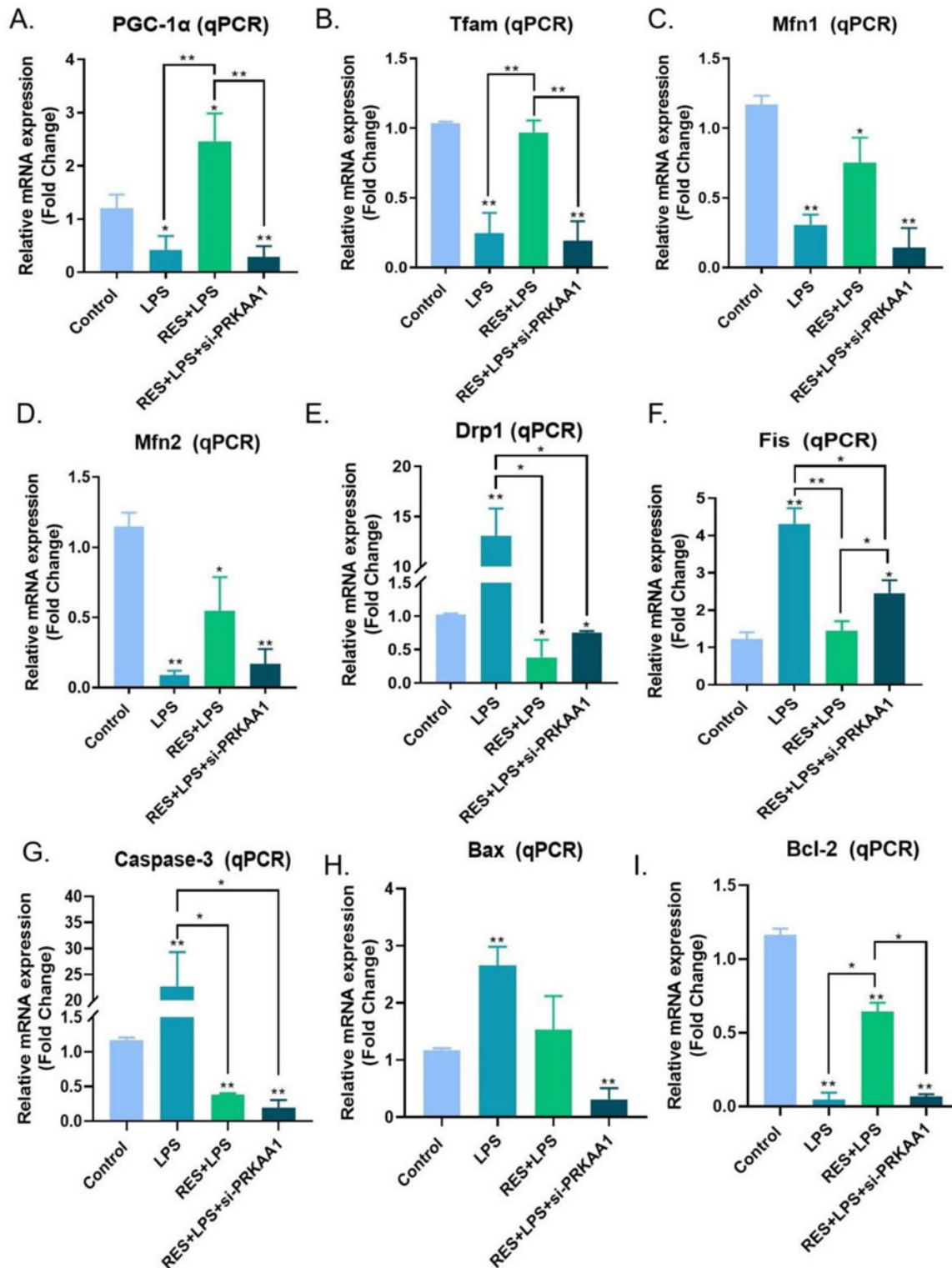


Figure 5. PRKAA1 mediates RES to regulate mitochondrial biosynthesis in BMECs induced by LPS, reduce mitochondrial damage and alleviate BMECs apoptosis. BMECs were treated with RES for 12 h and then treated with LPS for 12 h after the PRKAA1 interference fragment was transfected into BMECs for 24 h. A–I. The mRNA expression of PGC-1 α , Tfam, Mfn1, Mfn2, Drp1, Fis, Caspase-3, Bax, and Bcl-2 in the control, LPS, RES + LPS and RES + LPS + si-PRKAA1 groups, respectively. * $P < 0.05$, ** $P < 0.01$.

GSH-PX, Fig. 7C, $P < 0.05$) showed the opposite result with MDA. Simultaneously, mRNA levels of inflammatory factors (IL-6, IL-8, and IL-1 β) were detected, and we found that RES co-treatment

with LPS notably reduced their expression. However, the inhibitory effect of RES on inflammatory factors decreased after interfering with PRKAA1, in contrast to the control group (Fig. 7D–F,

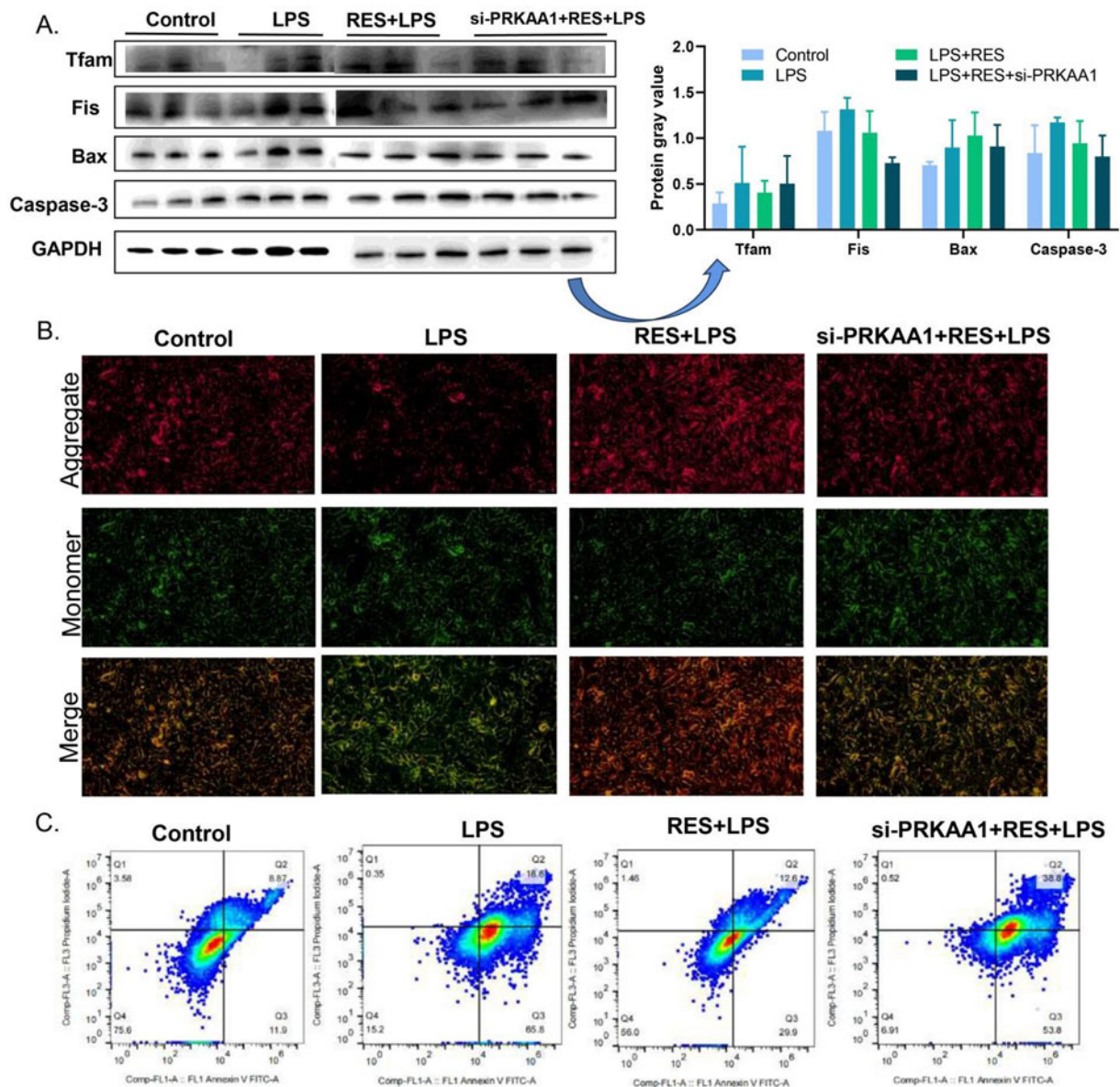


Figure 6. A. Western blot. B. Detection of mitochondrial membrane potential using JC-1. C. Apoptosis was detected using flow cytometry. Scale bar = 200 μ m.

$P < 0.01$). Similarly, the detection results of ROS showed that RES could inhibit the release of ROS from the BMECs induced by LPS, and the inhibition effects of RES was weakened after interfering with PRKAA1 (Fig. 7G, Supplementary Figure 2F).

Discussion

The mitochondrion is the energy center of cells and the center of pro-inflammatory response, playing an important role in the response against pathogenic infection (Andrieux et al. 2021). Mitochondrial dynamics play a central role in the process of pro-inflammatory signal transduction (Marchi et al. 2023). Research has shown that mitochondrial dysfunction promotes inflammatory responses. Moreover, retrograde signaling caused by dysfunctional mitochondria can alter gene expression, cell morphology and function, and mitochondrial kinetics may also play an important role in stress signaling. Normal mitochondria are highly dynamic

organelles whose size, shape, and network are controlled by cell physiology (Srinivasan et al. 2017). When mitochondrial integrity is compromised, mitochondrial damage-associated molecular patterns engage pattern recognition receptors, trigger inflammation, and promote pathology in an expanding list of diseases (West 2017).

Mitochondrial biogenesis refers to the process during which existing mitochondria produce new mitochondria. This biogenesis process is regulated by PGC-1 α , which is activated through phosphorylation or deacetylation, to further activate nuclear respiratory factors 1 and 2 (Nrf1 and Nrf2), and then activate mitochondrial Tfam (Li et al. 2017). Similarly, the expressions of PGC-1 α and Tfam were downregulated in vivo and in vitro in our experiment, which suggested that PGC-1 α had an activation disorder and mitochondrial biogenesis was disordered in mastitis cows. Tfam is a protein that participates in the transcription maintenance and replication of mitochondrial DNA (mtDNA); therefore, the

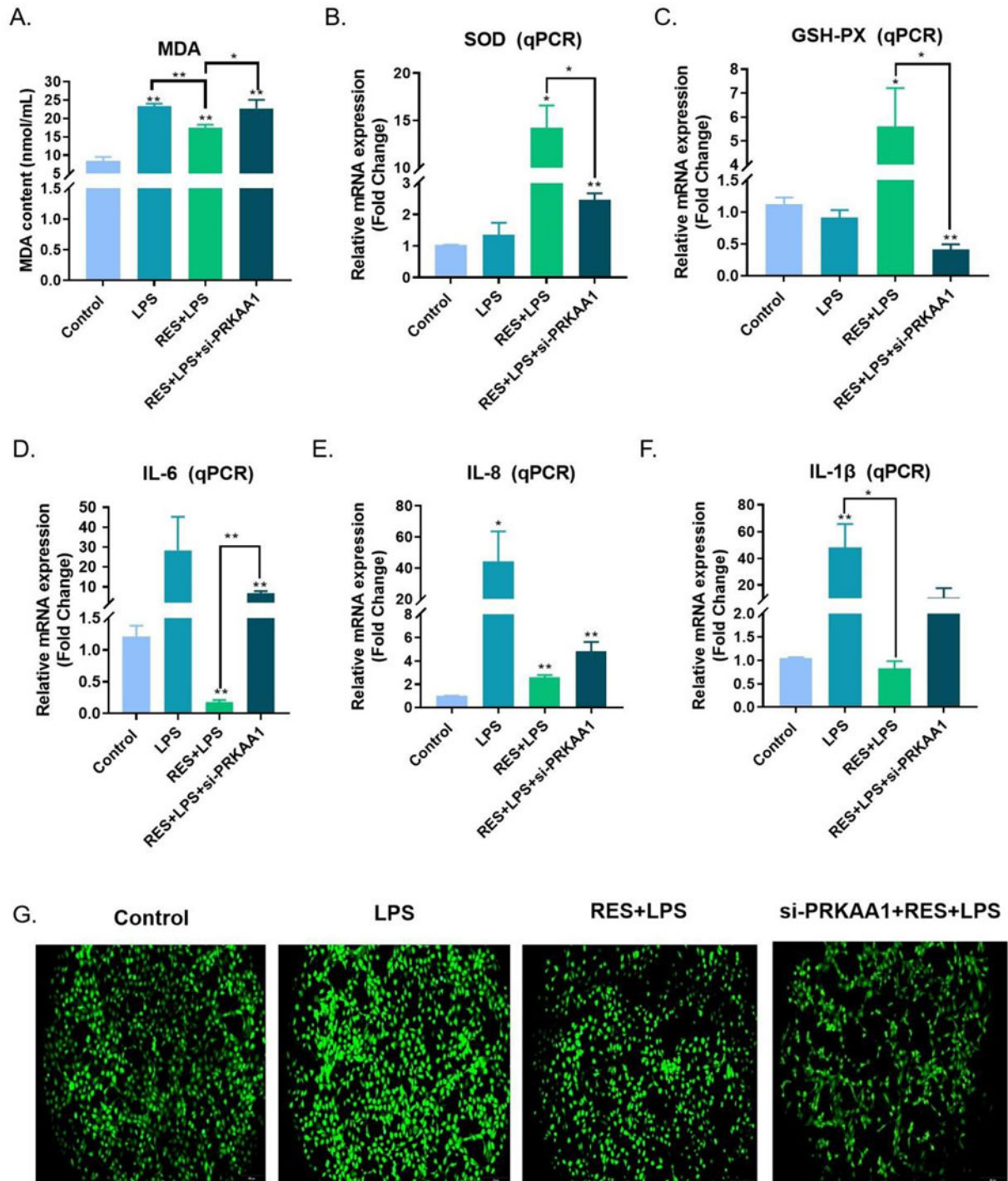


Figure 7. PRKAA1 mediates RES to reduce ROS production, improve antioxidant capacity and then alleviate inflammatory reaction in BMECs. A. MDA content. B–C. The mRNA expression of GSH-PX and SOD. D–F. The mRNA expression of IL-6, IL-8, and IL-1β. G. ROS production in BMECs detected by ROS detection kit. Scale bar = 200 μm. * $P < 0.05$, ** $P < 0.01$.

regulation of Tfam levels and PGC-1α activation can control the expression of mtDNA-encoded proteins, which, in turn, regulate mitochondrial biogenesis (Picca and Lezza 2015). Bi et al. (Bi et al. 2019) indicated that the addition of irisin to mouse hepatocytes promoted the expression of PGC-1α and Tfam, inhibited mitochondrial excessive division, promoted mitochondrial biogenesis and led to an increase in mitochondrial content to alleviate liver

injury. Resistin destroys mitochondrial biogenesis by inhibiting the PGC-1α/ Nrf1/Tfam signaling pathway. In human neuronal SH-SY5Y, Resistin destroys mitochondrial biogenesis by inhibiting the PGC-1α/ Nrf1/Tfam signaling pathway (Chen et al. 2018). The above results have shown that Tfam expression is similar to the parameters of mitochondrial biogenesis, which leads to the wide acceptance of Tfam as a marker of mitochondrial biogenesis.

mtROS reduced the abundance of mitochondrial Tfam in HK2 cells by suppressing its transcription and promoting Lon-mediated Tfam degradation, thus promoting mitochondrial dysfunction and inflammation (Zhao et al. 2021). The limitation of this experiment is that the ROS measured is the total ROS in the cells, whereas studies have shown that the ROS in the cells mainly comes from the mitochondrial respiratory chain, nicotinamide adenine dinucleotide phosphate (NADPH) oxidase, xanthine oxidase, and inflammation (Chen 2022; Sarniak et al. 2016). Similarly, mitochondrial damage is characterized by decreased metabolic activity, increased ROS production, membrane permeability changes and mitochondrial protein release into the cytoplasm, which increases intracellular oxidative stress. At a higher level of ROS, a longer mitochondrial permeability transition pore (mPTP) opening may release ROS explosion, leading to the destruction of mitochondria (Koch et al. 2017; Zorov et al. 2014). Mitosis is necessary for the generation of new mitochondria. Mitochondrial fission is crucial for controlling mitochondrial function, and Drp1 is the key mediator for mitochondrial division (Yang et al. 2022a). As the receptor of Drp1, Fis recruited Drp1 from the cytoplasm and formed a spiral around the mitochondria, then cut off the mitochondrial inner and outer membrane (Schmitt et al. 2018). Similarly, our nuclear and cytoplasmic localization of Drp1 and Fis also showed that they were mainly located in the cytoplasm. Yu et al. (Yu et al. 2020) found that LPS promotes the expression of signal transducer and transcriptional activator 2 and Drp1 in mouse macrophages, leading to mitochondrial division, while knocking out or inhibiting Drp1 reduces the increase in mitochondrial mass and pro-inflammatory differentiation. It was suggested that the upregulation of Drp1 promoted mitochondrial fission. Mfn1 and Mfn2, homologues of the fuzzy onion in yeast and drosophila, are key regulators of mitochondrial fusion in mammalian cells (Zhao et al. 2022). Mfn2 is a mitochondrial outer membrane protein that regulates mitochondrial fusion, while Mfn1 and Mfn2 act in three independent molecular complexes to promote mitochondrial fusion (Chen et al. 2003; Harland et al. 2020). Our research revealed that mRNA expression levels of Drp1 and Fis were elevated, whereas Mfn1 and Mfn2 expression levels were reduced in the blood of dairy cows suffering from mastitis, indicating that mitochondrial dynamics were in an imbalanced state and mitochondrial biogenesis was dysfunctional under the inflammatory state. Based on our findings, PRKAA1 is a key gene for RES to activate PGC-1 α , and PRKAA1 is involved in inflammation-related pathways, such as AMPK/PGC-1/SIRT1, mTOR, NF- κ B, which, in turn, provides a new idea for us to further explore the anti-inflammatory mechanism of PRKAA1-mediated RES.

RES is a non-flavonoid polyphenol organic substance with antioxidant, anti-inflammatory, and anti-cancer properties (Repossi et al. 2020), which can inhibit the mRNA expression of the toll-like receptor and pro-inflammatory genes, and its antioxidant activity and ability to inhibit the production of enzymes related to eicosanoid contribute to its anti-inflammatory properties (Capiralla et al. 2012). In addition, treatment with RES could inhibit the expression of tumor necrosis factor α (TNF α), IL-6 and IL-1 β . RES can be used as an activator of SIRT1, which can reduce the phosphorylation and acetylation of NF- κ B and the signal transducer and activator of transcription 1 (STAT1) by activating the SIRT3 signal, as well as weak Mn-induced oxidative stress and inflammatory cytokines (Cong et al. 2021). Our study found that RES can activate PGC-1 α via PRKAA1 to relieve inflammatory reaction in BMECs. PRKAA1, also known as AMPK α 1, is a catalytic subunit of AMPK and is crucial for regulating

cellular energy metabolism through phosphorylation (Zhang et al. 2020). It has been reported that the combined treatment of quercetin and RES reduced rat obesity and related inflammation induced by a high-fat diet through the AMPK α 1/SIRT1 signaling pathway, in addition, rats showed anti-inflammatory properties and anti-insulin resistance when administered alone or in combination (Zhao et al. 2017). RES acts as an activator of SIRT1, which, through activation of the SIRT3 pathway, reduces the phosphorylation and acetylation of NF- κ B and STAT1. This process also diminishes Mn-induced oxidative stress and the levels of inflammatory cytokines (Cong et al. 2021). RES activated the AMPK/PGC-1 α axis to promote obesity-damaged mitochondrial biogenesis and muscle regeneration, whereas the effect of RES was eliminated by AMPK α 1, which reversed the inhibition of PRKAA1 phosphorylation and SIRT1 expression, further confirming our research results (Zhao et al. 2017). The pro-mitochondrial fusion and anti-inflammatory functions of RES were significantly decreased after PRKAA1 intervention, suggesting that RES may regulate mitochondrial biogenesis through PRKAA1 activation of PGC-1 α , which may play an anti-inflammatory role. In our study, we found that RES application alone significantly increased the gene expression of PGC-1 α , Mfn1 and Mfn2, but the effect was slight when combined with LPS, for this result we hypothesized that LPS stimulation activates a strong inflammatory cascade, including the NF- κ B pathway, which can interfere with some of the beneficial effects of RES, especially in terms of mitochondrial gene expression. While RES is able to counteract the inflammation induced by LPS to some extent, it may not completely override the inflammatory suppression of mitochondrial biogenesis in this context. Mitochondrial damage is characterized by decreased metabolic activity, increased ROS production, membrane permeability changes, and mitochondrial protein release into the cytoplasm, which increases intracellular oxidative stress. At a higher level of ROS, a longer mPTP opening may release ROS explosion, leading to the destruction of mitochondria (Koch et al. 2017; Zorov et al. 2014). The massive release of ROS activates inflammatory corpuscles, which, in turn, promotes inflammation (Diebold and Chandel 2016). RES can also eliminate excessive ROS, increase the activity of SOD, enhance the potential and ATP levels of mitochondrial membranes, reduce the copy number of mtDNA and reduce the level of MDA. The increase of free radicals leads to the excessive production of MDA in cells, and the MDA level is usually regarded as a sign of oxidative stress and antioxidant status (Torun et al. 2009). Meanwhile, the research results showed that RES could promote mitochondrial biogenesis and function by activating the PGC-1 α signaling pathway (Zhou et al. 2021), which further confirms our experimental results. In this study, ROS content in BMECS was significantly increased and mitochondrial membrane potential was decreased in the inflammatory state. After addition of RES, ROS content was significantly reduced and mitochondrial damage was alleviated, but after PRKAA1 intervention, ROS content and mitochondrial membrane potential were not significantly different from those in the inflammatory group, indicating that PRKAA1 is an important target mediating RES anti-inflammation.

Conclusion

Taken together, PRKAA1 is the key gene that mediates the activation of PGC-1 α by RES, which regulates the mitochondrial biogenesis of mammary epithelial cells in dairy cows, inhibits ROS production, relieves mitochondrial damage, improves the antioxidant

capacity of BMECs, and then alleviates the inflammatory reaction of BMECs.

Supplementary material. The supplementary material for this article can be found at <https://doi.org/10.1017/anr.2024.27>.

Acknowledgements. Ningxia Ruminant Nutrition Science and Technology Innovation Team (No. 2024CXTD008, Yinchuan, China), Yinchuan Dairy Cow Health Breeding Science and Technology Innovation Team (No. 2023CXTD32, Yinchuan, China), Ningxia University Science and Technology Innovation Team (030700002417).

Author contributions. Data analysis, writing – original draft, Chunli Hu and Yanhao An.; data curation, software, Xuehu Ma.; review, editing, Xue Feng.; funding acquisition, project administration, review and editing, Yun Ma and Yanfen Ma. All authors read and approved the final version of the manuscript. ChunLi Hu and YanHao An authors are contributed equally to this work.

Conflicts of interest. The authors declare they have no competing financial interest and no conflict of interest.

Ethical standards and consent to participate. The experimental procedures were approved by the Animal Experiment Committee of Ningxia University according to the Regulations for the Administration of Affairs Concerning Experimental Animals in China (Ningxia University Ethics No. 22–72). The experimental procedures were strictly implemented according to the approved guidelines and regulations.

References

- Andrieux P, Chevillard C, Cunha-Neto E *et al.* (2021) Mitochondria as a cellular hub in infection and inflammation. *International Journal of Molecular Sciences* **22**, 11338.
- Annesley SJ and Fisher PR (2019) Mitochondria in Health and Disease. *Cells* **8**, 680.
- Ballou MA (2012) Growth and development symposium: Inflammation: Role in the etiology and pathophysiology of clinical mastitis in dairy cows. *Journal of Animal Science* **90**, 1466–1478.
- Bi J, Zhang J, Ren Y *et al.* (2019) Irisin alleviates liver ischemia-reperfusion injury by inhibiting excessive mitochondrial fission, promoting mitochondrial biogenesis and decreasing oxidative stress. *Redox Biology* **20**, 296–306.
- Capiralla H, Vingtdoux V, Zhao H *et al.* (2012) Resveratrol mitigates lipopolysaccharide- and Abeta-mediated microglial inflammation by inhibiting the TLR4/NF- κ B/STAT signaling cascade. *Journal of Neurochemistry* **120**, 461–472.
- Chen H, Detmer SA, Ewald AJ *et al.* (2003) Mitofusins Mfn1 and Mfn2 coordinately regulate mitochondrial fusion and are essential for embryonic development. *The Journal of Cell Biology* **160**, 189–200.
- Chen QM (2022) Nrf2 for protection against oxidant generation and mitochondrial damage in cardiac injury. *Free Radical Biology and Medicine* **179**, 133–143.
- Chen Z, Tao S, Li X *et al.* (2018) Resistin destroys mitochondrial biogenesis by inhibiting the PGC-1 α /NRF1/TFAM signaling pathway. *Biochemical and Biophysical Research Communications* **504**, 13–18.
- Cong L, Lei MY, Liu ZQ *et al.* (2021) Resveratrol attenuates manganese-induced oxidative stress and neuroinflammation through SIRT1 signaling in mice. *Food Chemistry and Toxicology* **153**, 112283.
- Das NR, Vaidya B, Khare P *et al.* (2021) Combination of peroxisome proliferator-activated receptor Gamma (PPAR γ) Agonist and PPAR Gamma co-activator 1 α (PGC-1 α) activator ameliorates cognitive deficits, oxidative stress, and inflammation in rodent model of Parkinson's disease. *Current Neurovascular Research* **18**, 497–507.
- Diebold L and Chandel NS (2016) Mitochondrial ROS regulation of proliferating cells. *Free Radical Biology and Medicine* **100**, 86–93.
- Eisele PS and Handschin C (2014) Functional crosstalk of PGC-1 coactivators and inflammation in skeletal muscle pathophysiology. *Seminars in Immunopathology* **36**, 27–53.
- Grive KJ and Sauerbrun-Cutler MT (2021) Resveratrol improves granulosa cell activity through mitochondrial biogenesis. *Fertil and Steril* **115**, 909–910.
- Harland M, Torres S, Liu J *et al.* (2020) Neuronal mitochondria modulation of LPS-induced neuroinflammation. *Journal of Neuroscience* **40**, 1756–1765.
- He L, Feng X, Hu C *et al.* (2024) HOXA9 gene inhibits proliferation and differentiation and promotes apoptosis of bovine preadipocytes. *BMC Genomics* **25**, 358.
- Hu C, Yang M, Feng X *et al.* (2024) miR-10167-3p targets TCF7L1 to inhibit bovine adipocyte differentiation and promote bovine adipocyte proliferation. *Genomics* **116**, 110903.
- Huang Q, Liu DH, Chen CF *et al.* (2021) Pgc-1 α promotes phosphorylation, inflammation, and apoptosis in H9c2 cells during the early stage of lipopolysaccharide induction. *Inflammation* **44**, 1771–1781.
- Jardim FR, de Rossi FT, Nascimento MX *et al.* (2018) Resveratrol and brain mitochondria: A review. *Molecular Neurobiology* **55**, 2085–2101.
- Koch RE, Josefson CC and Hill GE (2017) Mitochondrial function, ornamentation, and immunocompetence. *Biological Reviews of the Cambridge Philosophical Society* **92**, 1459–1474.
- Krishan S, Richardson DR and Sahni S (2014) Gene of the month. AMP kinase (PRKAA1). *Journal of Clinical Pathology* **67**, 758–763.
- Li L, Xiao L, Hou Y *et al.* (2016) Sestrin2 silencing exacerbates cerebral ischemia/reperfusion injury by decreasing mitochondrial biogenesis through the AMPK/PGC-1 α pathway in rats. *Scientific Reports* **6**, 30272.
- Li PA, Hou X and Hao S (2017) Mitochondrial biogenesis in neurodegeneration. *Journal of Neuroscience Research* **95**, 2025–2029.
- Li Z, Pan H, Yang J *et al.* (2023) Xuanfei Baidu formula alleviates impaired mitochondrial dynamics and activated NLRP3 inflammasome by repressing NF- κ B and MAPK pathways in LPS-induced ALI and inflammation models. *Phytomedicine* **108**, 154545.
- Ma YF, Wu ZH, Gao M *et al.* (2018) Nuclear factor erythroid 2-related factor 2-antioxidant activation through the action of ataxia telangiectasia-mutated serine/threonine kinase is essential to counteract oxidative stress in bovine mammary epithelial cells. *Journal of Dairy Science* **101**, 5317–5328.
- Malaguarrera L (2019) Influence of resveratrol on the immune response. *Nutrients* **11**, 946.
- Marchi S, Guilbaud E, Tait S *et al.* (2023) Mitochondrial control of inflammation. *Nature Reviews Immunology* **23**, 159–173.
- Meng T, Xiao D, Muhammed A *et al.* (2021) Anti-inflammatory action and mechanisms of resveratrol. *Molecules* **26**, 229.
- Missiroli S, Patergnani S, Caroccia N *et al.* (2018) Mitochondria-associated membranes (MAMs) and inflammation. *Cell Death and Disease* **9**, 329.
- Picca A and Lezza AM (2015) Regulation of mitochondrial biogenesis through TFAM-mitochondrial DNA interactions: Useful insights from aging and calorie restriction studies. *Mitochondrion* **25**, 67–75.
- Reposi G, Das UN and Eynard AR (2020) Molecular basis of the beneficial actions of resveratrol. *Archives of Medical Research* **51**, 105–114.
- Rius-Pérez S, Torres-Cuevas I, Millán I *et al.* (2020) PGC-1 α , inflammation, and oxidative stress: An integrative view in metabolism. *Oxid Med Cell Longev* **2020**, 1–20.
- Rong Y, Ren J, Song W *et al.* (2021) Resveratrol suppresses severe acute pancreatitis-induced microcirculation disturbance through targeting SIRT1-FOXO1 axis. *Oxidative Medicine and Cellular Longevity* **2021**, 8891544.
- Sarniak A, Lipinska J, Tytman K *et al.* (2016) Endogenous mechanisms of reactive oxygen species (ROS) generation. *Postępy Higieny I Medycyny Doświadczalnej (Online)* **70**, 1150–1165.
- Schmitt K, Grimm A, Dallmann R *et al.* (2018) Circadian control of DRP1 activity regulates mitochondrial dynamics and bioenergetics. *Cell Metabolism* **27**, 657–666.e5.
- Srinivasan S, Guha M, Kashina A *et al.* (2017) Mitochondrial dysfunction and mitochondrial dynamics-The cancer connection. *Biochimica Et Biophysica Acta Bioenergetics* **1858**, 602–614.
- Strandberg Y, Gray C, Vuocolo T *et al.* (2005) Lipopolysaccharide and lipoteichoic acid induce different innate immune responses in bovine mammary epithelial cells. *Cytokine* **31**, 72–86.

- Torun AN, Kulaksizoglu S, Kulaksizoglu M *et al.* (2009) Serum total antioxidant status and lipid peroxidation marker malondialdehyde levels in overt and subclinical hypothyroidism. *Clinical Endocrinology (Oxford)* **70**, 469–474.
- Waterhouse A, Bertoni M, Bienert S *et al.* (2018) SWISS-MODEL: Homology modelling of protein structures and complexes. *Nucleic Acids Research* **46**, W296–W303.
- West AP (2017) Mitochondrial dysfunction as a trigger of innate immune responses and inflammation. *Toxicology* **391**, 54–63.
- Whitley BN, Engelhart EA and Hoppins S (2019) Mitochondrial dynamics and their potential as a therapeutic target. *Mitochondrion* **49**, 269–283.
- Wilkins MR, Gasteiger E, Bairoch A *et al.* (1999) Protein identification and analysis tools in the ExpASY server. *Methods in Molecular Biology* **112**, 531–552.
- Xiao-Li W, Ting L, Ji-Hong L *et al.* (2017) The effects of resveratrol on inflammation and oxidative stress in a rat model of chronic obstructive pulmonary disease. *Molecules* **22**, 1529.
- Yang H, Sibilla C, Liu R *et al.* (2022a) Clueless/CLUH regulates mitochondrial fission by promoting recruitment of Drp1 to mitochondria. *Nature Communications* **13**, 1582.
- Yang J, Hu Q, Wang J *et al.* (2022b) RNA-seq reveals the role of miR-29c in regulating inflammation and oxidative stress of bovine mammary epithelial cells. *Frontiers in Veterinary Science* **9**, 865415.
- Yang Q, Ma Q, Xu J *et al.* (2022c) Endothelial AMPK α 1/PRKAA1 exacerbates inflammation in HFD-fed mice. *British Journal of Pharmacology* **179**, 1661–1678.
- Yu W, Wang X, Zhao J *et al.* (2020) Stat2-Drp1 mediated mitochondrial mass increase is necessary for pro-inflammatory differentiation of macrophages. *Redox Biology* **37**, 101761.
- Zandkarimi F, Vanegas J, Fern X *et al.* (2018) Metabotypes with elevated protein and lipid catabolism and inflammation precede clinical mastitis in prepartal transition dairy cows. *Journal Dairy Science* **101**, 5531–5548.
- Zhang Y, Zhou X, Cheng L *et al.* (2020) PRKAA1 promotes proliferation and inhibits apoptosis of gastric cancer cells through activating JNK1 and Akt pathways. *Oncology Research* **28**, 213–223.
- Zhao L, Cen F, Tian F *et al.* (2017) Combination treatment with quercetin and resveratrol attenuates high fat diet-induced obesity and associated inflammation in rats via the AMPK α 1/SIRT1 signaling pathway. *Experimental and Therapeutic Medicine* **14**, 5942–5948.
- Zhao M, Wang Y, Li L *et al.* (2021) Mitochondrial ROS promote mitochondrial dysfunction and inflammation in ischemic acute kidney injury by disrupting TFAM-mediated mtDNA maintenance. *Theranostics* **11**, 1845–1863.
- Zhao S, Heng N, Wang H *et al.* (2022) Mitofusins: From mitochondria to fertility. *Cellular and Molecular Life Sciences* **79**, 370.
- Zhou J, Yang Z, Shen R *et al.* (2021) Resveratrol improves mitochondrial biogenesis function and activates PGC-1 α pathway in a preclinical model of early brain injury following subarachnoid hemorrhage. *Frontiers in Molecular Biosciences* **8**, 620683.
- Zhou Y, Jin Y, Yu H *et al.* (2019) Resveratrol inhibits aflatoxin B1-induced oxidative stress and apoptosis in bovine mammary epithelial cells and is involved in the Nrf2 signaling pathway. *Toxicol* **164**, 10–15.
- Zhu H, Foretz M, Xie Z *et al.* (2014) PRKAA1/AMPK α 1 is required for autophagy-dependent mitochondrial clearance during erythrocyte maturation. *Autophagy* **10**, 1522–1534.
- Zorov DB, Juhaszova M and Sollott SJ (2014) Mitochondrial reactive oxygen species (ROS) and ROS-induced ROS release. *Physiological Reviews* **94**, 909–950.